Journal of Electronics, Electromedical Engineering, and Medical Informatics
Homepage: jeeemi.org; Vol. 7, No. 4, October 2025, pp: 1130-1143 e-ISSN: 2656-8632

RESEARCH ARTICLE OPEN ACCESS

MCRNET-RS: Multi-Class Retinal Disease Classification using Deep Learning-based Residual Network-Rescaled

Mohana Suganthi N, and Arun M

Department of Computer Science and Engineering, Vel Tech Rangarajan Dr. Sagunthala R&D Institute of Science and Technology, Avadi, Chennai, Tamil Nadu, India.

Corresponding author: Mohana Suganthi N. (e-mail: mohanasuganthin@veltech.edu.in), **Author(s) Email**: Arun M. (e-mail: drarunm@veltech.edu.in)

Abstract **Retinal diseases are a major cause of vision impairment, leading to partial or complete blindness if undiagnosed. Early detection and accurate classification of these conditions are crucial for effective treatment and vision preservation. However, Conventional diagnostic techniques are time-consuming and require professional assistance. Additionally, existing deep-learning models struggle with feature extraction and classification accuracy because of differences in image quality and disease severity. To overcome these challenges, a novel deep learning (DL)-based MCRNET-RS approach is proposed for multi-class retinal disease classification using fundus images. The gathered fundus images are pre-processed using the Savitzky-Golay Filter (SGF) to enhance and preserve essential structural details. The DL-based Residual Network-Rescaled (ResNet-RS) is used to extract hierarchical feature extraction for accurate retinal disease classification. Multi-layer perceptron (MLP) is used to classify retinal diseases such as Diabetic Neuropathy (DN), Branch Retinal Vein Occlusion (BRVO), Diabetic Retinopathy (DR), Healthy, Macular Hole (MH), Myopia (MYA), Optic Disc Cupping (ODC), Age-Related Macular Degeneration (ARMD), Optic Disc Pit (ODP), and Tilted Superior Lateral Nerve (TSLN). The effectiveness of the proposed MCRNET-RS method was assessed using precision, recall, specificity, F1 score, and accuracy. The proposed MCRNET-RS approach achieves an overall accuracy of 98.17%, F1 score of 95.99% for Retinal disease classification. The proposed approach improved the total accuracy by 3.27%, 4.48%, and 4.28% compared to EyeDeep-Net, Two I/P VGG16, and IDL-MRDD, respectively. These results confirm that the proposed MCRNET-RS framework provides a strong, scalable, and highly accurate solution for automated retinal disease classification, thereby supporting early diagnosis and effective clinical decision-making.**

Keywords **Retinal diseases; deep learning; Savitzky-Golay filtering; Multi-Layer Perceptron; ResNet-Rescaled**.

I. Introduction

Retinal disorders are a prevalent problem in older adults, causing impaired vision and even vision loss as the eye's ability to function is weakened. The photosensitive layer of the retina is a thin structure inside the eye. Blurred vision and, in rare cases, complete vision loss are symptoms of retinal disease [1]. These diseases impair vision, leading to partial or complete blindness if left untreated. AMD, DR, retinal detachment, and retinitis pigmentosa are common retinal conditions [2]. Each of these conditions affects the retina differently, causing symptoms such as blurry vision, dark spots, distorted images, and loss of peripheral or central vision [3]. Retinal diseases are caused by factors such as genetics, aging, diabetes, hypertension, and lifestyle choices. Diagnostic methods of conventional eye diseases are time-consuming and require specialized knowledge [4], [5]. It is critical to detect retinal diseases early and initiate treatment as soon as possible to preserve vision and manage them. An early diagnosis is achieved with the aid of Fluorescein angiography, fundus imaging, retinal imaging, and optical coherence tomography (OCT) [6],[7]. Several treatment options are available for this condition, such as medications, laser therapy, vitrectomy, and intravitreal injections [8].

Advanced DL models are increasingly used to assist in early diagnosis and treatment planning, improving patient outcomes [9]. Deep learning [10] has transformed the medical imaging sector analysis, offering highly accurate and automated solutions for detecting and classifying retinal diseases [11]. CNN and cutting-edge designs like Attention UNet [12], Transformer-based models, and GAN have

Manuscript Received 20 July 2025; Revised 10 September 2025; Accepted 20 September 2025; Available online 29 September 2025
Digital Object Identifier (**DOI**): https://doi.org/10.35882/jeeemi.v7i4.925

significantly improved the ability to analyze retinal images from OCT, fluorescein angiography, and fundus photography [13]. These models automatically extract complex features, detect subtle abnormalities, and highly precise classify diseases like DR, ARMD, and glaucoma [14]. DL models enhance early diagnosis, reducing the need for manual intervention and improving clinical decision-making [15].

Retinal conditions such as ARMD, DR, and retinal detachment result in irreparable vision loss if they are not detected in time. Traditional diagnosis takes longer and is less accessible in rural areas since it depends on experts [16]. The progressive nature of these illnesses sometimes results in late detection, which diminishes therapy effectiveness. Automated and accurate diagnostic procedures are becoming increasingly important to improve early diagnosis and timely treatment [17]. Advanced imaging and DL enhance diagnosis, improving the efficiency and accessibility of treating eye conditions [18]. To overcome these issues, a novel Retinal disease classification model is proposed in this research. The primary contributions of the MCRNET-RS approach are summarized as follows:

1. The proposed DL-based model effectively detects and classifies retinal diseases with high accuracy, enhancing diagnostic efficiency and facilitating early disease detection.
2. SGF improves image quality by preserving structural details to ensure better feature extraction and classification performance.
3. ResNet-RS is utilized for hierarchical feature extraction and visualizing the representation of retinal diseases for improved classification accuracy.
4. The MLP efficiently processes the extracted features to accurately classify multi-class retinal diseases, improving diagnostic precision and reliability.

The following sections of this work are organized as follows: Section 2 presents a summary of the Retinal disease literature survey. Section 3 describes the MCRNET-RS approach in detail. Section 4 discusses the results and discusses the MCRNET-RS. Section 5 concludes the work and offers suggestions for future research.

II. Literature Survey

DL and machine learning (ML) methods have been developed in recent years to detect and classify Retinal disease. This section discusses some of the relevant studies. A non-invasive automated DL approach to identify numerous eye illnesses using colour fundus images introduced in 2023 Sengar, N., et al., [19]. Multi-class fundus images were retrieved dataset and several augmentation approaches were utilized framework robust in real-time.

Sarki et al. (2021) proposed a CNN [20] based on deep learning for the multi-classification of diabetic eye illness. The suggested method's maximum accuracy, sensitivity, and specificity for classification using multiple classes were 81.33%, 96%, and 97%, respectively. They provide an interdependent model for retinal fundus images that learns the characteristics of the fundus image. A CNN with four pre-trained CNN architectures and two distinct optimizers was developed by Gour and Khanna [21]. It is based on transfer learning. They concluded that the SGD optimizer pre-trained on the VGG16 model of ocular illnesses is the best architecture for multi-class, fundus picture classification. In 2020, DL-based automatic detection of mild and diabetic sickness with several classes. The experiment used two CNN models that had previously been trained on ImageNet was introduced by Sarki, R., et al., The intermediate multi-class classification accuracy of the VGG16 technique was 85.95% [22]. For the various classifications of retinal illnesses, Gualsaqui, M.G., et al. [23] introduced a CNN approach based on DL in 2023. The VGG16 architecture was determined to have the greatest outcomes in terms of accuracy and loss after each architecture was analyzed.

Using fundus images, T. Vaiyapuri et al. designed IDL-MRDD, [24] a deep learning-based system for detecting multiple retinal diseases. The proposed paradigm aims to classify colour fundus images into a number of classifications, such as AD, DR, Hypertensive Retinopathy, Glaucoma, Normal, Pathological, and Others. The experimental values outperformed the existing techniques with a maximum accuracy of 0.963. A DL-based method for classifying retinal diseases using OCT images was presented by Kim and Tran et al. [25]. To create the binary classifiers, a number of CNNs, including feature extractors, have been used. Changes have been made to InceptionV3, DenseNet121, ResNet50, ResNet152, VGG16, and VGG19. The Normal class binary classifier experimental result shows an accuracy of 0.999.

Existing methods in the literature review have many shortcomings that limit their effectiveness in retinal disease classification. While deep learning models like CNN, VGG16, and SSAE have shown promise, they often struggle with feature extraction, reducing accuracy in detecting subtle retinal abnormalities. Some approaches lack robustness to variations in image quality, illumination, and disease severity, affecting their generalization across diverse datasets. To overcome these challenges, a novel MCRNET-RS approach accurately classifies Retinal diseases, enhancing diagnostic efficiency and improving early disease detection.

Manuscript Received 20 July 2025; Revised 10 September 2025; Accepted 20 September 2025; Available online 29 September 2025
Digital Object Identifier (**DOI**): https://doi.org/10.35882/jeeemi.v7i4.925

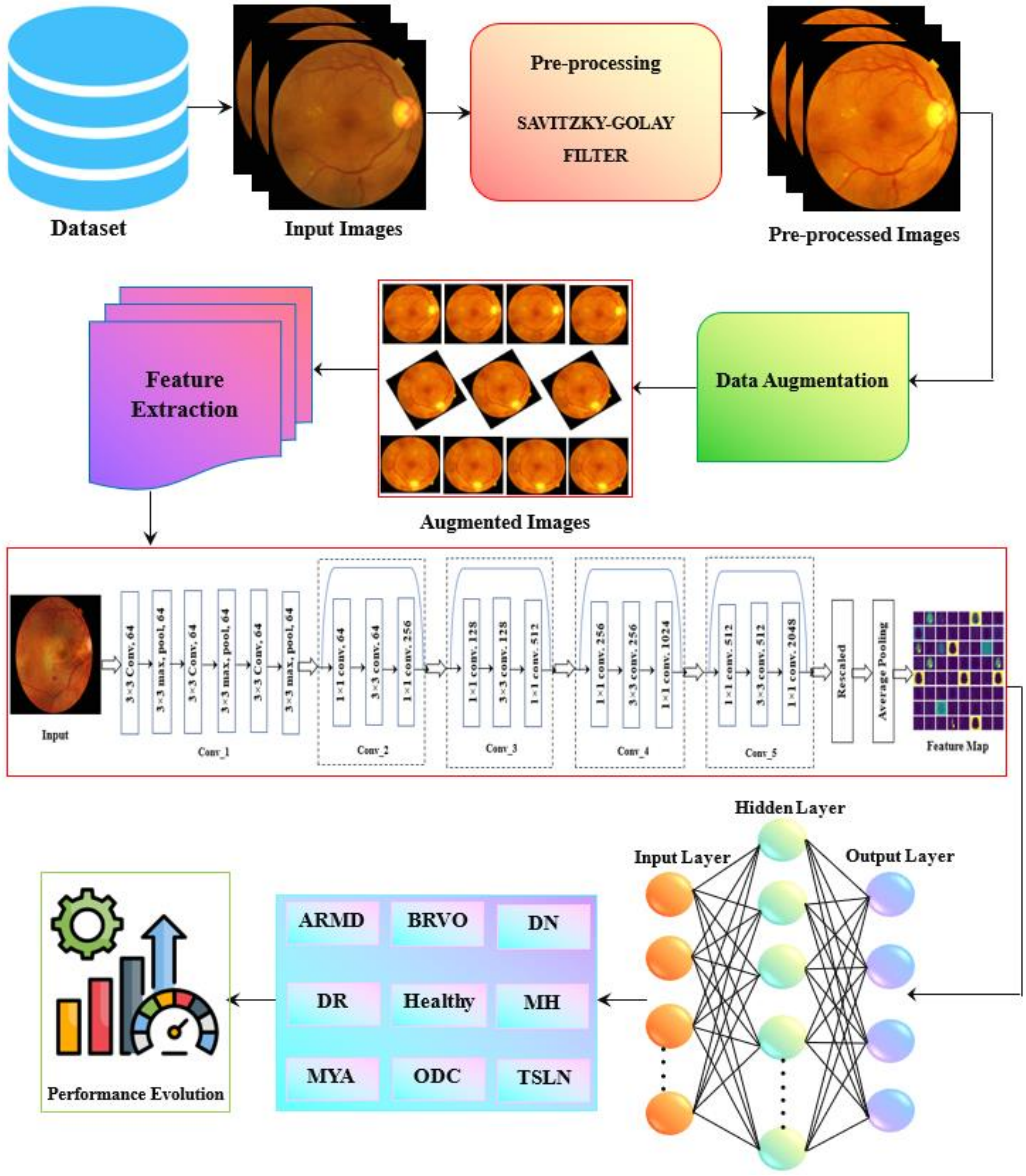

Fig.1. The proposed MCRNET-RS mode

III. Methodological Framework

This research proposes a novel MCRNET-RS approach for classifying Retinal disease from the RFMiD dataset. Fig. 1 demonstrates the workflow of the MCRNET-RS approach.

A. Dataset Acquisition

The Retinal Fundus Multi-Disease Image Dataset (RFMiD) is openly accessible [29]. It is specifically created for the classification of multi-class retinal diseases. It consists of 3,200 high-resolution fundus images collected from real-world clinical settings covering 46 different retinal conditions such as hypertensive retinopathy, ARMD, glaucoma, and DR. The dataset was split into 80% for training and 20% for testing to evaluate the performance of the MCRNET-RS model. Stratified sampling was utilized to maintain proportional representation of all 10 disease classes. The proposed MCRNET-RS approach was evaluated using 3-fold and 5-fold cross-validation. Each fold preserved the class distribution to align with best practices in multi-class retinal image classification. This validation strategy helps to minimize overfitting and provides a more reliable estimation of the approach's performance across various data subsets. The dataset includes expert-labeled annotations, and it is highly diverse, featuring a wide range of disease severities, image qualities, and variations in patient demographics.

Manuscript Received 20 July 2025; Revised 10 September 2025; Accepted 20 September 2025; Available online 29 September 2025
Digital Object Identifier (**DOI**): https://doi.org/10.35882/jeeemi.v7i4.925

Table 1. Distribution of Retinal Disease Classes in the RFMiD Dataset

S. no	Classes	No. of images
1	ARMD	169
2	BRVO	119
3	DN	230
4	DR	632
5	Healthy	669
6	MH	523
7	MYA	167
8	ODC	445
9	ODP	115
10	TSLN	304

Table 1 presents the distribution of retinal fundus images across different disease classes in the RFMiD dataset, which comprises 3,372 images. The dataset covers 10 categories, including pathological conditions such as ARMD, BRVO, DR, and MYA, along with healthy cases. The Healthy class contains the highest number of images, 669, while the ODP class has the fewest, 115. This dataset provides a balanced yet diverse representation of common and rare retinal diseases.

Table 2. Dataset Distribution Before and After Augmentation

Classes	Before Augmentation	After Augmentation
ARMD	169	600
BRVO	119	600
DN	230	600
DR	632	600
Healthy	669	600
MH	523	600
MYA	167	600
ODC	445	600
ODP	115	600
Total	3,372	6,000

Table 2 presents the distribution of image samples within the retinal disease classes before and after data augmentation. Initially, the RFMiD dataset exhibited a degree of class imbalance, with certain classes like Healthy (669) and DR (632) having significantly more samples compared to minority classes such as ODP (115) and BRVO (119). This imbalance model's performance leads to biased predictions toward the majority classes. To address this, data augmentation techniques were applied to increase the number of samples in underrepresented classes synthetically . After augmentation, each class was balanced to 600 images, creating a uniform distribution across all 10 disease categories. This balanced dataset significantly contributed to the high per-class sensitivity and specificity observed in the results, ensuring that the model learned robust features from each class without bias.

A. Pre-processing using SGF

The Savitzky-Golay filter (SGF) is used to smooth retinal images while preserving essential structural details by enhancing image quality for better disease analysis. An SGF, also known as a Savitzky-Golay smoother, is a special low-pass filter to smooth a noisy signal. SGF operates as a time-domain smoothing filter using the least squares method to successive subsets of neighboring data points; a low-degree polynomial is fitted. For this implementation, a window size of 7×7 pixels was chosen with a second-order polynomial kernel, which effectively smooths noise while maintaining edge sharpness. This kernel size was selected after empirical testing on validation images to balance noise reduction with detail preservation. The choice of a 7×7 window provided sufficient local context to smooth intensity variations without over-smoothing small pathologies. The parameters were optimized using visual inspection, histogram evaluation, and early-stage validation accuracy.

Let the width of the filter window be $w = 2s + 1$, where s is the half-window size. Let the length of the unique signal be w is the width of the filter window length of the unique signal be N, and the measurements point be $(X = X_{-s}, X_{-s+1}, \dots, X_0, \dots, X_{s-1}, X_s)$. A polynomial fit is performed on the window signal using an i-th degree polynomial present in Eq. (1) [26].

$$y = a_0 + a_1 x + a_2 x^2 + \cdots + a_i x^i \quad (1)$$

where w is the form a system of i- element linear equations $(w > i + 1)$. The least squares approach is applied to determine the fitting parameters $[a_0, a_1, \dots, a_i]$ and solve the system of Eq. (2) [26].

$$\begin{bmatrix} y_{-s} \\ \vdots \\ y_0 \\ \vdots \\ y_s \end{bmatrix} = \begin{bmatrix} 1 & (x_{-s})^1 & \dots & (x_{-s})^{\frac{i}{2}} & \dots & (x_{-s})^i \\ \vdots & \vdots & \vdots & \vdots & \vdots & \vdots \\ 1 & (x_0)^1 & \dots & (x_0)^{\frac{i}{2}} & \dots & (x_0)^i \\ \vdots & \vdots & \vdots & \vdots & \vdots & \vdots \\ 1 & (x_{s+1})^1 & \dots & (x_s+1)^{\frac{i}{2}} & \dots & (x_{s+1})^i \end{bmatrix} \begin{bmatrix} a_0 \\ \vdots \\ a_{\frac{i}{2}} \\ \vdots \\ a_i \end{bmatrix} + \begin{bmatrix} e_{-s} \\ \vdots \\ 0 \\ \vdots \\ e_s \end{bmatrix} \quad (2)$$

Transform the above system of equations into a matrix expression, Eq. (3) [26].

$$Y_{(2s+1)\times 1} = X_{(2s+1)\times k} \cdot A_{k\times 1} + E_{(2s+1)\times k} \quad (3)$$

Manuscript Received 20 July 2025; Revised 10 September 2025; Accepted 20 September 2025; Available online 29 September 2025
Digital Object Identifier (**DOI**): https://doi.org/10.35882/jeeemi.v7i4.925

The least squares solution is performed to obtain the most appropriate solution of $\tilde{A}$ Eq. (4) [26].

$$\tilde{A} = (X^T.X)^{-1}.X^T.Y \quad (4)$$

Substituting the resulting $\tilde{A}$ and M back into the matrix expression yields the most appropriate predicted value $\tilde{y}$ within the window illustrated in Eq. (5) [26]:

$$\tilde{y} = M.A = M.(X^T.X)^{-1}.M^T.Y = B.Y \quad (5)$$

The above method achieves data smoothing and feature point aggregation. It shows that different window sizes have different effects on image enhancement. A window too small will not highlight the color features of the image, while a window too large will make the image too blurred. This SGF approach effectively smooths retinal images while retaining critical features, aiding in accurate disease detection.

B. Feature extraction via ResNet-RS

ResNet-RS is used to extract hierarchical features from retinal images for accurate analysis and disease classification. The ResNet-RS is utilized a compound scaling strategy, adjusting depth, width, and resolution for optimal performance. The network comprises 50 layers with bottleneck residual blocks, each consisting of 1×1, 3×3, and 1×1 convolution. Identity shortcuts are used to enable gradient flow and avoid vanishing gradients. Transfer learning was employed by initializing the network with ImageNet pre-trained weights to enhance convergence. This configuration ensures efficient extraction of multi-scale retinal features while maintaining computational efficiency. ResNet-RS is an improved version of ResNet designed to achieve better performance while maintaining computational efficiency. Traditional ResNet architectures scale by increasing depth, which often leads to diminishing returns due to optimization challenges. ResNet-RS introduces a systematic way of scaling, ensuring optimal usage of model capacity without excessive computational overhead. Fig. 2 illustrates the architecture of the proposed ResNet-RS.

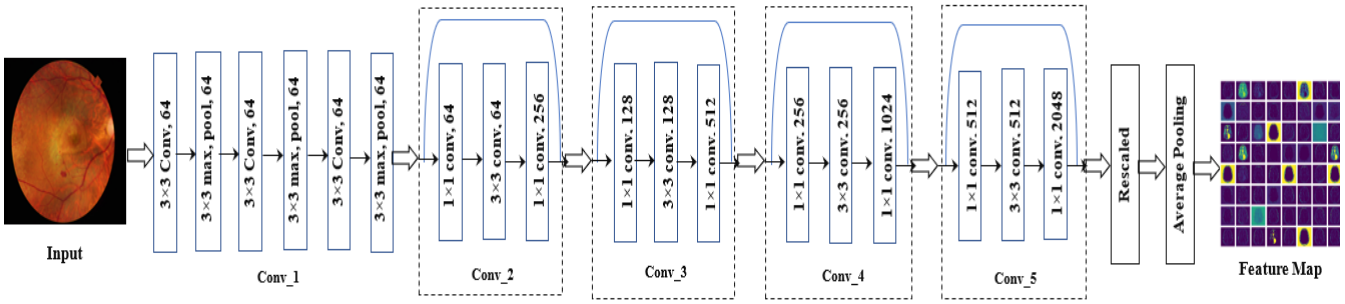

Fig. 2. Architecture of proposed ResNet-RS

ResNet-RS is an enhanced version of the original ResNet architecture, optimized for both accuracy and computational efficiency through a compound scaling strategy. While standard ResNet networks increase model depth to improve performance, ResNet-RS simultaneously scales depth (d), width (w), and input resolution (r) in a balanced manner. This allows the model to better utilize its capacity without drastically increasing computational cost or risking overfitting. The compound scaling is governed by Eq. (6) [27]:

$$d = \alpha^{\emptyset}, \quad w = \beta^{\emptyset}, \quad r = \gamma^{\emptyset} \quad (6)$$

Where $\alpha, \beta, and\ \gamma$ constants found through grid search, and φ is a user-defined scaling coefficient. In this work, we adopt ResNet-RS-50, a base configuration with 50 convolutional layers. To enhance learning capacity, the width is scaled to 1.2× the base configuration, and the input resolution is increased from 224×224 to 256×256, which enables better capture of fine retinal structures crucial for disease classification.

ResNet-RS follows the bottleneck architecture of ResNet. Each block consists of three convolutions: a 1×1 conv reduces the number of channels, a 3×3 conv. Feature extraction and 1×1 conv to restore dimensions. Mathematically, the bottleneck block is expressed as Eq. (7) [27]:

$$y = x + f\left(R_3.\sigma\left(R_2.\sigma(R_1.x)\right)\right) \quad (7)$$

Where x is the input feature map R_1, R_2, R_3 are weight matrices, σ represents a non-linearity and f is the residual function that applies batch normalization and activation, and y is the final output of the operation. ResNet-RS enhances retinal image analysis by efficiently extracting hierarchical features while maintaining computational efficiency. These enhancements collectively ensure more accurate and generalizable feature extraction, essential for reliable multi-class retinal disease classification.

C. Classification using MLP

Multilayer Perceptron (MLP) is used to classify the retinal disease ARMD, BRVO, DN, DR, Healthy, MH, MYA, ODC, ODP, and TSLN. MLP is a kind of ANN made up of several node layers. The MLP classifier comprises three hidden layers, each with 128, 64, and 32 neurons. Each layer introduces non-linearity

Manuscript Received 20 July 2025; Revised 10 September 2025; Accepted 20 September 2025; Available online 29 September 2025
Digital Object Identifier (**DOI**): https://doi.org/10.35882/jeeemi.v7i4.925

using the ReLU activation function. To lessen overfitting, a dropout rate of 0.5 is implemented following each hidden layer. The output layer classifies many classes using the softmax activation function across 10 retinal disease classes. This approach uses categorical cross-entropy loss for training and the Adam optimizer for optimization. Fig. 3 illustrates the MLP structure for Retinal disease classification.

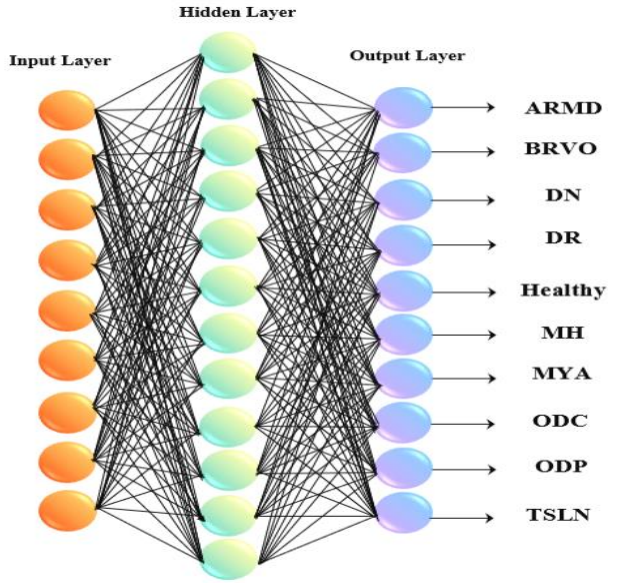

Fig. 3. Structure of Multi-layer Perceptron

The fundamental unit of an MLP is the perceptron, which introduces non-linearity by applying an activation function and calculating the inputs weighted sum. Mathematically a given neuron j, the output is given Eq. (8) [28]:

$$z_j = \sum_{i=1}^{n} w_{ji} x_i + b_j \quad (8)$$

where x_i represents the input w_{ji} represents the weight assigned to every input connection and a_j is the bias term. This weighted sum goes through an activation function after that f like the tanh function, ReLU or sigmoid Eq. (9) [28]:

$$a_j = f(z_j) \quad (9)$$

An MLP with multiple layers are mathematically represented using matrix notation. Given an input vector X and weight matrices W, the output of a layer written as Eq. (10) [28]:

$$M^{(l)} = f(W^{(l)} M^{(l-1)} + N^{(l)}) \quad (10)$$

where $M^{(l)}$ symbolizes the layer activations $l, W^{(l)}$ is the layer's weight matrix l, and $N^{(l)}$ is the bias vector. This MLP approach classifies Retinal disease types by extracted features to achieve precise classification. To avoid overfitting, a dropout rate of 0.5 was applied within the MLP layers, and a learning rate of 0.0001 with step decay was used. The consistent performance across cross-validation folds confirms that the model generalizes well without signs of overfitting.

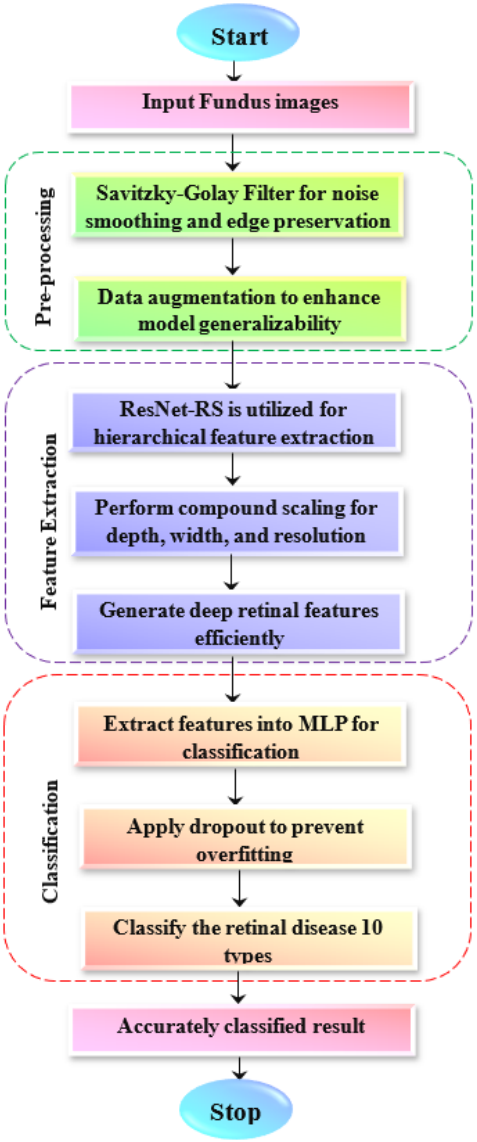

Fig. 4. Flow chart of the proposed MCRNET-RS method

Fig. 4 illustrates the workflow of the proposed MCRNET-RS method for multi-class retinal disease classification. The input fundus images are processed in the preprocessing stage, where the Savitzky-Golay Filter is applied for noise reduction and edge preservation, and data augmentation is performed to enhance model generalizability. In the feature extraction phase, ResNet-RS is utilized to capture hierarchical deep features, leveraging compound scaling for depth, width, and resolution to generate retinal features efficiently. These features are then passed to an MLP through the classification stage, where dropout is applied to mitigate overfitting. Finally,

Manuscript Received 20 July 2025; Revised 10 September 2025; Accepted 20 September 2025; Available online 29 September 2025
Digital Object Identifier (**DOI**): https://doi.org/10.35882/jeeemi.v7i4.925

the model classifies the retinal images into 10 distinct disease categories, producing accurate classification results.

Table 3. Hyperparameter Setting of the Proposed Model

Hyperparameter	Value
Framework	MATLAB 2020b
Hardware	NVIDIA RTX 3090 GPU
Dataset	RFMiD
Feature Extraction	ResNet-RS
Classifier	MLP
Learning Rate	0.0001
Batch Size	32
Number of Epochs	100
Dropout	0.5
Cross-Validation	3-Fold and 5-Fold
Learning Rate	0.0001

Table 3 demonstrates the training parameters of the MCRNET-RS approach. The approach was implemented using MATLAB 2020b and trained on the RFMiD dataset for multi-class retinal disease classification. ResNet-RS architecture was utilized for hierarchical feature extraction, and the MLP was utilized to classify retinal disease types. Training was conducted using a learning rate of 0.0001, a batch size of 32, and a total of 100 epochs. A dropout of 0.5 was applied to prevent overfitting, and the categorical cross-entropy loss function. The learning rate was scheduled using a step decay mechanism. Experiments were executed on an NVIDIA RTX 3090 GPU to ensure computational efficiency and robustness.

IV. Result

This section details the experimental results of the MCRNET-RS approach. The proposed MCRNET-RS model was implemented using MATLAB 2020b, leveraging the Deep Learning Toolbox for model construction and training. Custom scripts were developed for preprocessing and visualization tasks. Additionally, GPU acceleration was enabled through the Parallel Computing Toolbox to speed up training on an NVIDIA RTX 3090. This setup ensures reproducibility for researchers using MATLAB-based environments.

The proposed MCRNET-RS approach was assessed using several metrics, including accuracy, specificity, F1 score, precision, and recall, depending on images taken from the RFMiD dataset. The

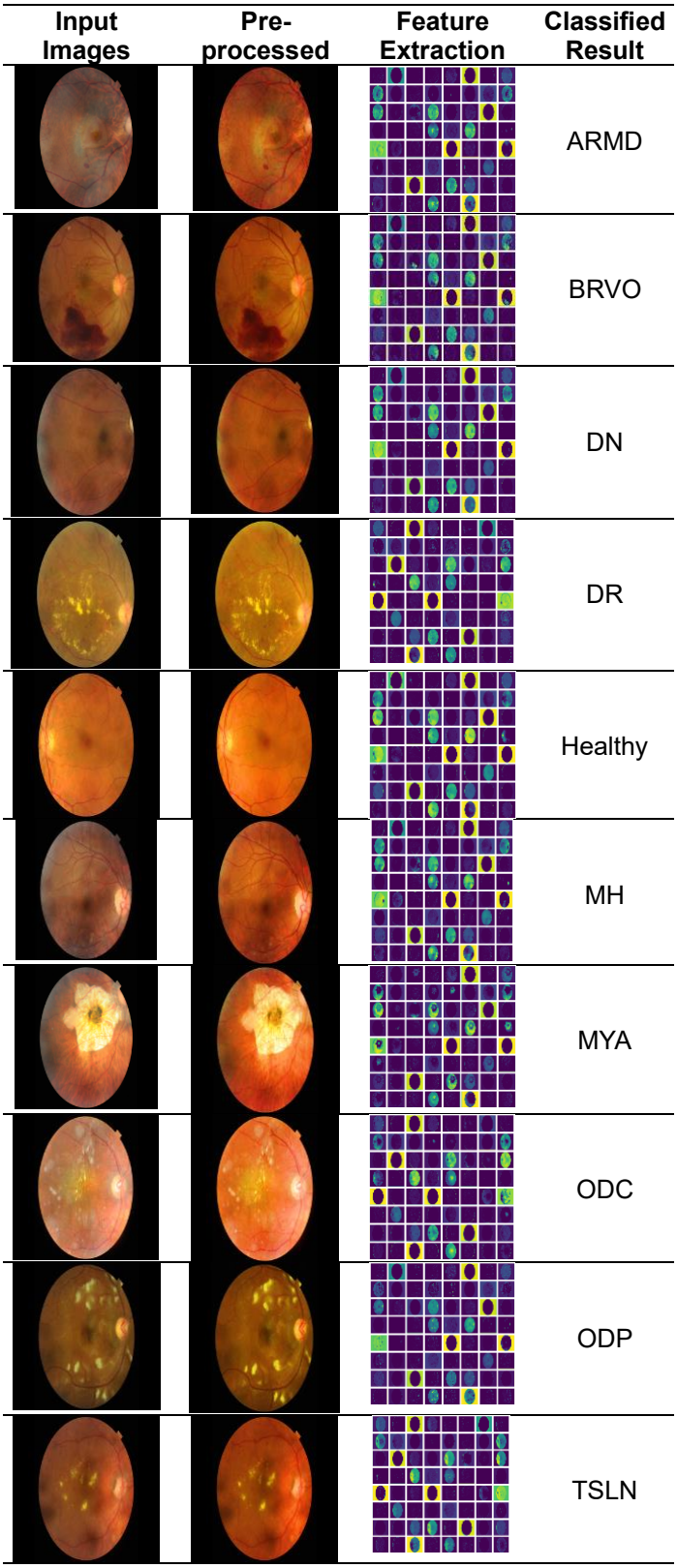

Fig. 5. Experimental result of MCRNET-RS approach

Manuscript Received 20 July 2025; Revised 10 September 2025; Accepted 20 September 2025; Available online 29 September 2025
Digital Object Identifier (**DOI**): https://doi.org/10.35882/jeeemi.v7i4.925

experimental results of the MCRNET-RS model for retinal disease are demonstrated in Fig. 5.

A. Performance analysis

The MCRNET-RS approach was evaluated in this section utilizing several metrics such as specificity (sp), F1 score, accuracy (ac), precision (pr), and recall (rc), on the gathered RFMiD dataset. SP evaluates the model accuracy in identifying negative situations. It computed by separating the total number of negatives by the number of correctly predicted negatives Eq. (11) [20]:

$$SP = \frac{T_{neg}}{T_{neg}+F_{pos}} \quad (11)$$

PR calculates the percentage of optimistic forecasts that come true. It emphasizes the capacity of the model to reduce false positives Eq. (12) [20]:

$$PR = \frac{T_{pos}}{T_{pos}+F_{pos}} \quad (12)$$

RE evaluates the approach capacity to accurately detect every real positive case. It is the proportion of all actual positive observations to correctly displayed positive observations Eq. (13) [20]:

$$RE = \frac{T_{pos}}{T_{pos}+F_{neg}} \quad (13)$$

AC calculates the predictions made by the model overall. It is computed as the proportion of accurately predicted samples to all samples, Eq. (14) [20]:

$$AC = \frac{T_{pos}+T_{neg}}{Total\ no.of\ samples} \quad (14)$$

F1 represents the harmonic mean of PR and RE, offering a balanced measure when there is an uneven class distribution, Eq. (15) [20]:

$$F1 = 2\left(\frac{Precision+Recall}{Precision+Recall}\right) \quad (15)$$

The DI is a similarity measure used to gauge the overlap between two sets, often used in image segmentation to compare the segmentation with the ground truth. Where T_{neg} and T_{pos} specifies true negatives and true positives of the sample images, F_{neg} and F_{pos} specifies false negatives and false positives of the sample images.

Fig. 5 presents the experimental result of the proposed MCRNET-RS approach. The transformation from raw retinal input images utilized to smoothed outputs using SGF. Then, hierarchical feature extraction using ResNet-RS, and finally, MLP is used to classify the retinal disease, namely ARMD, BRVO, DN, DR, Healthy, MH, MYA, ODC, ODP, and TSLN. Each stage reflects the model's ability to progressively refine progressively and SGF. Then, hierarchical feature extraction using ResNet-RS, and finally, MLP is used to classify the retinal disease, namely ARMD, BRVO, DN, DR, Healthy, MH, MYA, ODC, ODP, and TSLN. Each stage reflects the model's ability to progressively refine and process visual features for accurate retinal disease detection.

Table 4. Performance analysis of the MCRNET-RS approach

Types	AC%	SP%	PR%	RE%	F1%
ARMD	98.37	97.40	95.32	96.38	98.02
BRVO	98.76	98.11	94.65	98.30	97.21
DN	97.83	96.32	94.22	95.81	96.89
DR	99.12	98.97	96.37	98.42	99.04
Healthy	99.55	99.21	97.94	95.39	98.27
MH	98.79	93.64	96.53	94.70	95.34
MYA	96.36	91.80	94.37	93.94	92.95
ODC	97.29	96.68	95.83	93.69	97.12
ODP	98.88	97.46	95.21	96.48	94.22
TSLN	96.79	94.36	93.43	92.65	90.89

Table 4 presents the specificity, F1score, accuracy, recall, and precision of the proposed approach for classes with several levels. Table 1 presents the efficiency metrics of the proposed approach for the classes listed below: ARMD, BRVO, DN, DR, Healthy, MH, MYA, ODC, ODP, and TSLN. The accuracy of the proposed approach is 98.37% for ARMD, 98.76% for BRVO, 97.83% for DN, 99.12% for DN, 99.55% for Healthy, 98.79% for MH, 96.36 % for MYA, 97.29% for ODC, 98.88% for ODP, and 96.79% for TSLN, respectively. The MCRNET-RS approach achieves a total accuracy rate of 98.17%. These results indicate strong diagnostic potential for real-world retinal screening. However, variability in image quality,

Manuscript Received 20 July 2025; Revised 10 September 2025; Accepted 20 September 2025; Available online 29 September 2025
Digital Object Identifier (**DOI**): https://doi.org/10.35882/jeeemi.v7i4.925

unseen conditions, and clinical workflow integration remain key challenges. The overall accuracy of the MCRNET-RS model is highly effective across all classes, highlighting its strong performance. This is largely attributed to the robust hierarchical feature extraction capability of ResNet-RS, which effectively captures both fine-grained and global retinal features essential for accurate diagnosis. Notably, challenging classes such as ODC and ODP achieved high F1 scores of 97.12% and 94.22%, respectively, demonstrating the model's strong generalization ability. In Fig. 6, the accuracy curve displays over 100 epochs, showing the y-axis and x-axis. Based on the epochs, the proposed MCRNET-RS training and testing accuracy curve displays a high accuracy level of 98.17%. The loss curve achieves a smaller loss of 1.83%, indicating that the MCRNET-RS model works effectively throughout both the training and testing stages.

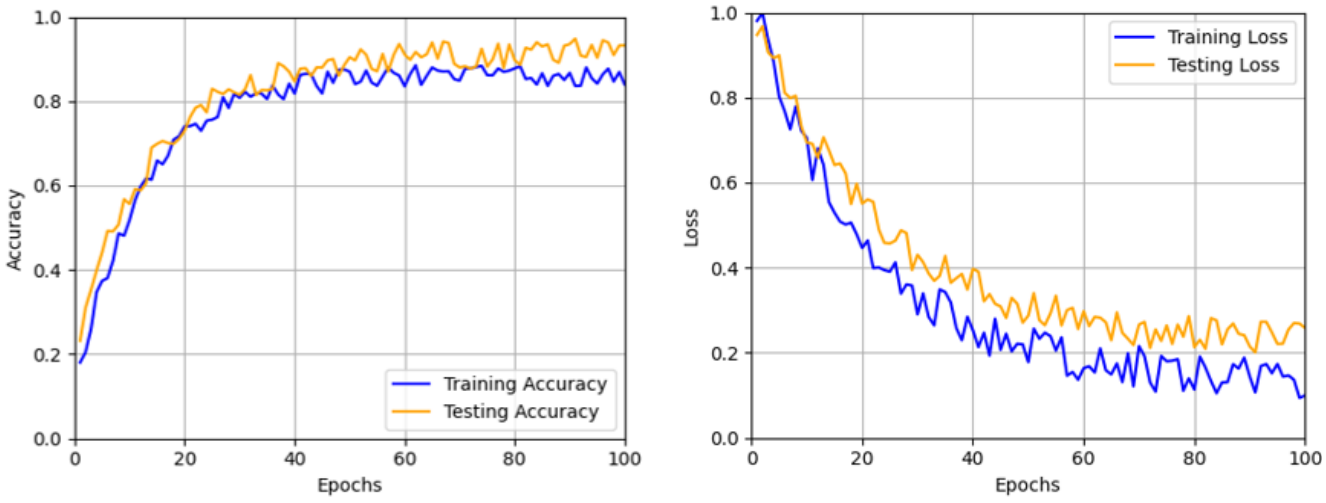

(a) (b)

Fig. 6. The curve of the MCRNET-RS of (a) Accuracy and (b)Loss

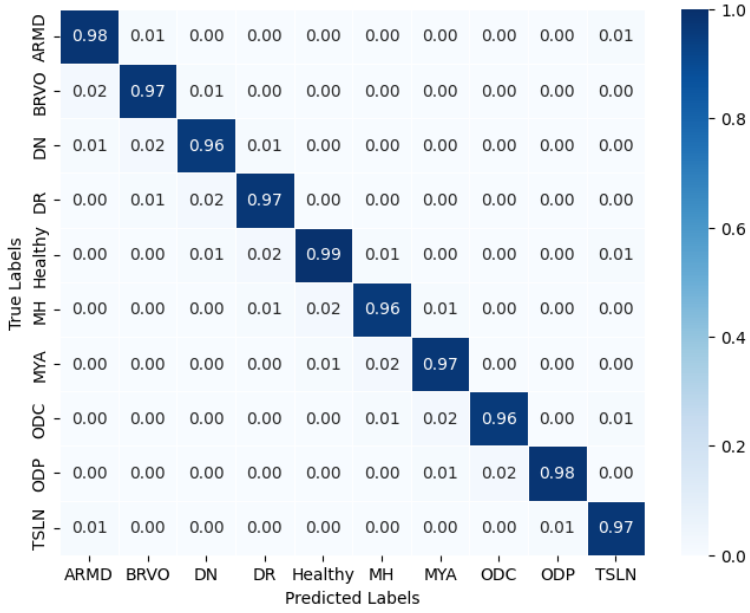

Fig. 7. Confusion matrix for MLP

Fig 7 presents the confusion matrix for the Retinal disease classification performance of a model across types of Retinal, namely ARMD, BRVO, DN, DR, Healthy, MH, MYA, ODC, ODP, and TSLN. The diagonal elements near 1 show that the model properly classifies most samples and shows a high accuracy for

Manuscript Received 20 July 2025; Revised 10 September 2025; Accepted 20 September 2025; Available online 29 September 2025
Digital Object Identifier (**DOI**): https://doi.org/10.35882/jeeemi.v7i4.925

most classes. The values indicate accurate predictions on the diagonal, whereas the off-diagonal numbers indicate misclassifications. For Healthy, the suggested MLP achieved a high accuracy of 0.99%. Strong performance is demonstrated by this MLP method classifier, which achieves excellent classification accuracy across all classes.

Fig. 8 illustrates the ROC curve for the MCRNET-RS method based on the performance of various metrics. The MCRNET-RS method of retinal disease classification for Healthy individuals achieves a high AUC of 99.28. The ROC curves show that the proposed approach produces high results using the retinal disease class, yielding the highest AUC value.

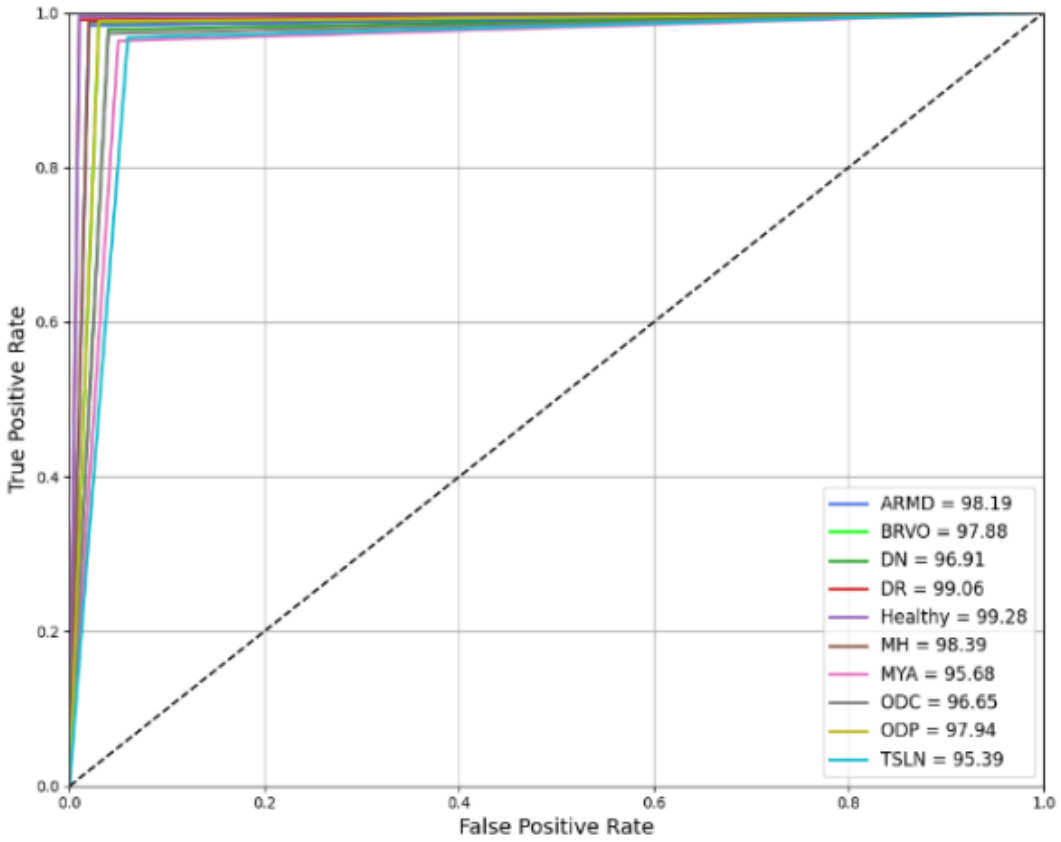

Fig.8. ROC curve of the proposed MCRNET-RS method

The performance of the MCRNET-RS method was assessed using 3-fold and 5-fold cross-validation techniques to strengthen and generalize it. The dataset was split into respective folds, and the results were averaged across all runs using both cross-validation methods, as illustrated in Table 5.

Table 5. Cross-validation results of the proposed model

Metric	3-Fold Cross-Validation	5-Fold Cross-Validation
Accuracy	98.23%	98.10%
Precision	96.87%	96.14%
Recall	96.44%	95.92%
F1-score	97.65%	96.03%
Specificity	96.89%	95.86%

Table 5 shows the MCRNET-RS model cross-validation results using 3-fold and 5-fold methods. In the 3-fold cross-validation, three subsets of the data are used, 40% of which are utilized for training in each fold, and the remaining 20% for testing. For the 5-fold cross-validation, the data is separated into five subgroups, with 20% of each subset being utilized for testing and 20% for training. These evaluations confirm the proposed model's stability and high generalization ability across different validation strategies.

B. Comparative analysis

In this section, the proposed MLP approach is contrasted with several current methods based on efficiency indicators. Effectiveness is measured based on precision, recall, accuracy, F1 score, and specificity. The efficiency of the MCRNET-RS model is compared with three existing techniques, CNN [20], VGG16 [21], and SSAE [24], for classifying retinal disease.

Manuscript Received 20 July 2025; Revised 10 September 2025; Accepted 20 September 2025; Available online 29 September 2025
Digital Object Identifier (**DOI**): https://doi.org/10.35882/jeeemi.v7i4.925

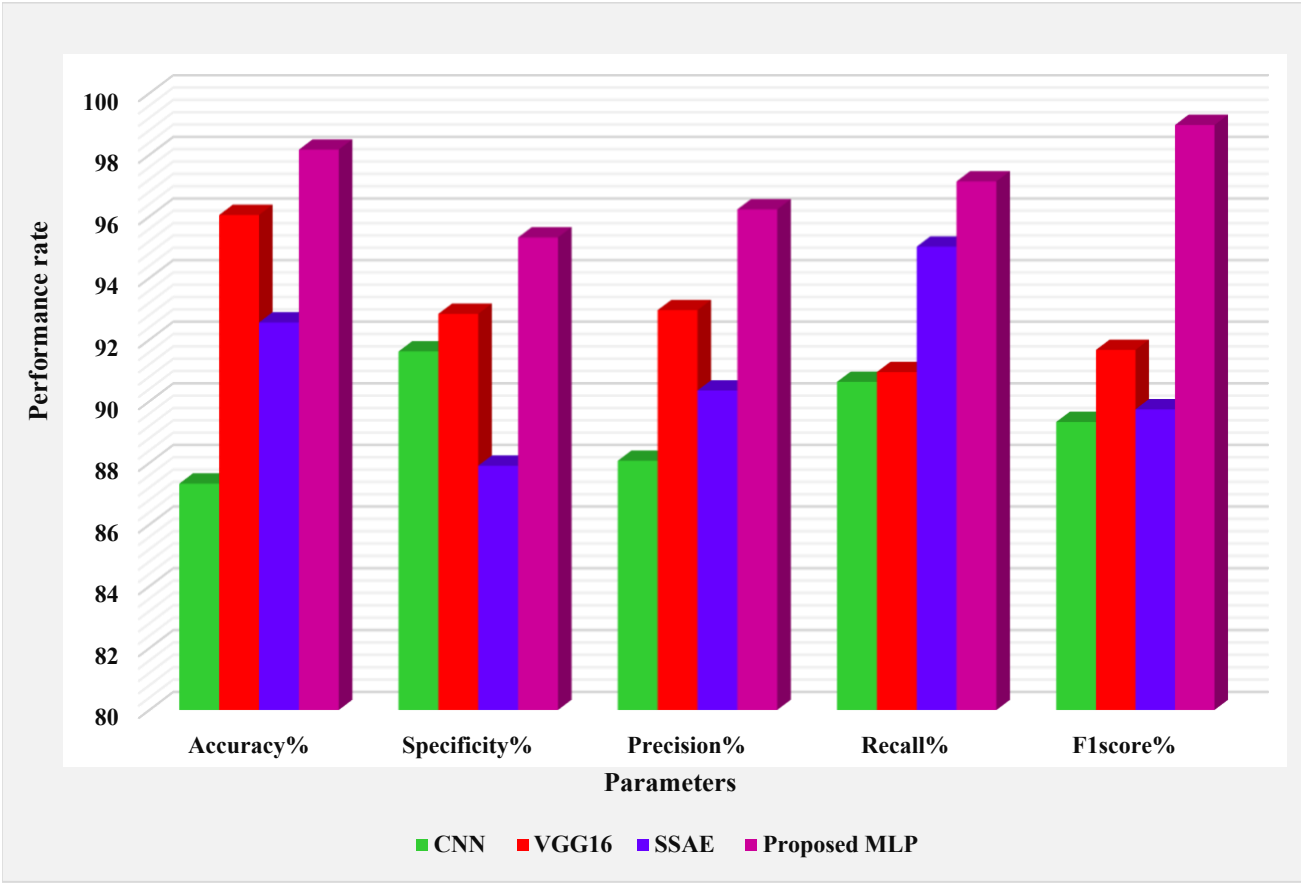

Fig. 9. Comparison of existing DL networks and proposed network

Table 6. Comparison of the proposed method with existing methods

Techniques	AC%	PR%	F1%	SP%	RE%	p-value
CNN	87.33	88.07	89.33	91.62	90.63	0.042
VGG16	96.05	92.96	91.67	92.84	90.95	0.037
SSAE	92.56	90.35	89.74	87.91	95.02	0.040
Proposed MLP	98.17	96.23	98.97	95.32	97.14	0.029

Table 6 compares the accuracy obtained by the proposed MCRNET-RS and existing techniques such as CNN, VGG16, and SSAE. The proposed model performs 12.41%, 2.20%, and 6.06% better than the conventional approaches such as CNN, VGG16, and SSAE for Retinal disease classification. Fig. 9 shows CNN, VGG16, and SSAE are 87.33%, 96.05%, and 92.56% respectively. The reported p-values from paired t-tests are all below 0.05, indicating that the performance improvements of MCRNET-RS are statistically significant compared to existing approaches. The MCRNET-RS achieves better results than existing networks, with an accuracy rate of 98.17% for the classification of retinal disease.

Table 7 presents a comparison of existing datasets and the proposed dataset. The RFMiD dataset outperforms others with the highest accuracy of 98.17%. Messidor, DIARETDB1, and EyePACS datasets show slightly lower accuracies of 95.06%, 93.96%, and 94.14%. The proposed model clearly demonstrates the superior capability of the RFMiD dataset in supporting high-accuracy multi-class retinal disease classification.

V. Discussion

The experimental results demonstrate that the proposed MCRNET-RS model achieves a superior performance in multi-class retinal disease classification of 98.17%. This notable improvement over existing DL

Manuscript Received 20 July 2025; Revised 10 September 2025; Accepted 20 September 2025; Available online 29 September 2025
Digital Object Identifier (**DOI**): https://doi.org/10.35882/jeeemi.v7i4.925

Table 7. Comparison between the proposed dataset and the existing datasets

Dataset	Accuracy%	Precision%	F1 score%
Messidor	95.06	94.20	94.60
DIARETDB1	93.96	92.80	93.10
EyePACS	94.14	93.45	93.75
RFMiD (Ours)	98.17	96.23	98.97

approaches such as CNN of 87.33%, VGG16 of 96.05%, and SSAE of 92.56%. Initially, integrating of the SGF technique significantly enhanced fundus image quality by improving contrast and preserving fine structural details, enabling the detection of small lesions and subtle abnormalities. Then ResNet-RS was a backbone with its compound scaling strategy, effectively capturing fine-grained local patterns and global retinal features ensuring strong discrimination between visually similar disease categories. MLP classifier incorporating dropout regularization and a sensibly tuned learning rate provided strong generalization capability. This is demonstrated by the consistent performance across 3-fold 98.23% and 5-fold 98.10% cross-validation. Furthermore, class-wise evaluation Table 4 shows that even challenging categories such as Optic Disc Pit (ODP) and Tilted Superior Lateral Nerve (TSLN) achieved high F1-scores of 94.22% and 90.89% indicating that the model generalizes well across both common and rare disease classes

Table 8. Comparison of existing approaches and proposed approach

Authors	Techniques	AC
A. Geetha., et al., (2025) [2]	Deep GD	92.47%
BDK. Patro., (2024) [16]	Vision Transform	96.69%
Sengar, N., et al., (2023) [19]	EyeDeep-Net	95.06%
MG. Gualsaqui, (2023) [23]	Multi-Class CNN	93.96%
Vaiyapuri, T., et al., (2022) [24]	IDL-MRDD	94.14%
Proposed	MCRNET-RS	98.17%

Table 8 illustrates the comparative analysis between the proposed MCRNET-RS model and existing models. The proposed MCRNET-RS achieves a higher accuracy of 98.17%, outperforming the existing models by margins of 6.16%, 1.53%, 3.27%, 4.48%, and 4.28%, respectively. A key similarity among these approaches is their reliance on CNN-based architectures for feature extraction. The performance is constrained by limited scalability, reduced robustness to class imbalance, or fewer disease categories. In contrast, integrating a compound-scaled ResNet-RS in the proposed model efficiently balances depth, width, and resolution, leading to superior hierarchical feature representation. Furthermore, as shown in Table 8, while Deep GD [2], EyeDeep-Net [19], Multi-Class CNN [23], and IDL-MRDD [24] achieved accuracies that the proposed model clearly surpassed. Interestingly, although the Vision Transformer [16] reported 96.69% accuracy higher than traditional CNN, it still fell short compared to MCRNET-RS, demonstrating the advantages of combining Savitzky-Golay preprocessing with compound scaling and balanced augmentation. Notably, existing EyeDeep-Net [19] and IDL-MRDD [24], which struggled with class imbalance or fewer categories, the proposed MCRNET-RS effectively classified ten disease categories, including rare cases such as ODP and TSLN, with high consistency. These gains are statistically significant ($p < 0.05$), confirming that integrating SGF preprocessing with the ResNet-RS backbone enhances feature quality and improves stability and generalization, enabling reliable classification across a wide range of retinal disease presentations.

The strong performance of several limitations needs to be acknowledged. Initially, the evaluation was conducted exclusively on the RFMiD dataset. However, diversity may not fully capture variations in real-world settings, such as differences in camera models, resolutions, and lighting conditions. Then the model's clinical applicability has not yet been validated through deployment in real patient-care environments. Ungradable images, patient movement, and varied

Manuscript Received 20 July 2025; Revised 10 September 2025; Accepted 20 September 2025; Available online 29 September 2025
Digital Object Identifier (**DOI**): https://doi.org/10.35882/jeeemi.v7i4.925

clinical protocols may affect performance. The model demonstrates strong classification accuracy, but the current implementation lacks comprehensive explainability mechanisms. Finally, the rare classes like BRVO and ODP performed well in controlled testing; their low real-world prevalence could present challenges when scaling the model to large, heterogeneous screening populations.

The high accuracy, generalization capability, and multi-class handling ability of the proposed MCRNET-RS model have important implications for clinical practice. It could serve as a reliable early screening tool in primary healthcare centers, particularly in rural or resource-limited settings where access to trained ophthalmologists is scarce. By integrating the model into tele-ophthalmology platforms can enable remote triage and prioritize high-risk patients for timely specialist referral. The ability to simultaneously detect multiple retinal conditions makes it a strong candidate for inclusion in comprehensive eye-health screening programs, potentially reducing diagnostic delays and improving patient outcomes. Moreover, the underlying architecture extended into multimodal frameworks, combining fundus images with other patient health data, such as OCT scans, for more holistic ocular disease prediction. These applications position MCRNET-RS as a promising foundation for next-generation AI-assisted ophthalmic diagnostic systems.

VI. Conclusion

This research proposed the DL-based MCRNET-RS model for multi-class retinal disease classification using fundus images. The collected fundus images were pre-processed with the SGF for image enhancement and preserving essential structural details. The ResNet-RS is utilized to extract hierarchical features for accurate retinal disease classification. MLP is used to classify retinal disease: ARMD, BRVO, DN, DR, Healthy, MH, MYA, ODC, Optic Disc Pit ODP, and TSLN. The MCRNET-RS approach achieves % overall accuracy of 98.17% for Retinal disease classification. The MCRNET-RS approach increased the overall accuracy by 3.27%, 4.48%, and 4.28% better than EyeDeep-Net, Two I/P VGG16, and IDL-MRDD, respectively. The MCRNET-RS model demonstrates high accuracy and robustness but is limited by its evaluation solely on the RFMiD dataset, which may not capture real-world variations such as diverse imaging devices, lighting conditions, and unseen disease types. Future work will validate the MCRNET-RS model on multi-center datasets with diverse imaging conditions.

Acknowledgment

The author would like to express his heartfelt gratitude to the supervisor for his guidance and unwavering support during this research for his guidance and support.

Funding

Not applicable.

Data Availability

The datasets used in this study are publicly available from the RIADD (Retinal Image Analysis for multi-Disease Detection) Challenge, hosted on the Grand Challenge platform. The training, evaluation, and test datasets each comprising 46 class labels can be accessed via the official RIADD download page: https://riadd.grand-challenge.org/download-all-classes/

Author Contribution

Mohana Suganthi N conceptualized and designed the study, conducted data collection, and participated in data analysis and interpretation. Arun M contributed to the educational media's development, oversaw the intervention's implementation, and contributed to manuscript writing and revisions. Mohana Suganthi N, and Arun M assisted with data analysis and interpretation and provided critical feedback on the manuscript. All authors reviewed and approved the final version of the manuscript, and agreed to be responsible for all aspects of the work ensuring integrity and accuracy.

Declarations

Ethical Approval

My research guide reviewed and ethically approved this manuscript for publication in this Journal.

Consent for Publication Participants.

Not applicable.

Competing Interests

This paper has no conflict of interest for publication.

References

[1] H. Hammoud, MY. Al Aref, M. Al Jabouli, M. Hammoud, W. Shehieb, and K. Arshad, “AI-Based Primary Diagnosis of Ocular Health via Smartphone,” In 2024 17th *International Conference on Signal Processing and Communication System (ICSPCS)*, *IEEE,* pp.1-5, 2024, doi: 10.1109/icspcs63175.2024.10815827

[2] A. Geetha, M.C. Sobia, D. Santhiand, and A. Ahilan, “DEEP GD: Deep learning based snapshot ensemble CNN with EfficientNet for glaucoma detection,” *Biomed. Signal Process. Control., vol*. 100, pp. 106989. 2025, doi: 10.1016/j.bspc.2024.106989

Manuscript Received 20 July 2025; Revised 10 September 2025; Accepted 20 September 2025; Available online 29 September 2025
Digital Object Identifier (**DOI**): https://doi.org/10.35882/jeeemi.v7i4.925

[3] A. Bindhu, A. Ahilan, S. Vallisree, P. Maria Jesi, B. Muthu Kumar, N.K Marriwala, and AQM. Sabr, "Skin Cancer Diagnosis Using High-Performance Deep Learning Architectures," *In International Conference on Emergent Converging Technologies and Biomedical Systems*, pp. 693-703, 2023, doi: 10.1007/978-981-99-8646-0_54

[4] P.T. Karule, S.B. Bhele, P. Palsodkar, P.T. Agarkar, H.R. Hajare, and P.R. Patil, "Detection of Multi-Class Multi-Label Ophthalmological Diseases in Retinal Fundus Images Using Machine Learning," In 2024 International Conference on Innovations and Challenges in Emerging Technologies (ICICET), *IEEE,* pp. 1-6, 2024.

[5] S. Caroline, and V.S. Lakshmi Harshitha, "Deep-Fir: Deep Learning based Butterfly Optimized Regression Network for Fast Image Retrieval", *International Journal of Data Science and Artificial Intelligence*, vol. 02, no.05, pp. 149-154, 2024.

[6] R. Kala, R. Chandrasekaran, A. Ahilan, and P. Jayapriya, "Brain Magnetic Resonance Image Inpainting via Deep Edge Region-based Generative Adversarial Network," *Journal of Electrical Engineering & Technology,* pp.1-12, 2024, doi: 10.1007/s42835-024-02025-0

[7] C. John Clementsingh, and S. Sumathi, "Face Regeneration and Recognition using Deep Learning based Sift-Hog Assisted Gan Model," *International Journal of Data Science and Artificial Intelligence,* vol. 02, no.05, pp. 142-148. 2024.

[8] R. Ingle, CK. Selvi, A. Ahilan, N. Muthukumaran, S. Sharma, and M. Kumar, "SERAV Deep-MAD: deep learning-based security–reliability–availability aware multiple D2D environment," *IETE J. Res*, pp.1-14, 2024, doi: 10.1080/03772063.2024.2415502

[9] M. Dhipa, Christopher John Clement Singh, E. Michael Priya, and T. Shunmugavadivoo, "Deep Learning-Based Classification of Lichens in Western Ghats using Aerial Images," *International Journal of Computer and Engineering Optimization,* vol. 02, no. 01, pp. 14-19, 2024.

[10] K.R. Akhila, N. Muthukumaran, and A. Ahilan, "Classification of cervical cancer using an autoencoder and cascaded multilayer perceptron," *IETE Journal of Research,* vol. 70, no. 1, pp.26-36, 2024, doi: 10.1080/03772063.2022.2142859

[11] T.S. Chandrakantha, B.N. Jagadale, G.R. Madhuri, and T.E. Abhishek, "AI in Ophthalmic Imaging: Enhancing Retina Analysis for Early Disease Detection," In 2024 IEEE International Conference on Computer Vision and Machine Intelligence (CVMI), IEEE, pp. 1-6, 2024, doi: 10.1109/cvmi61877.2024.10782114

[12] Arun Ramaiah, Parvathi Devi Balasubramanian, Ahilan Appathurai, Narayan Aperumal Muthukumaran, "Detection of Parkinson's Disease Via Clifford Gradient-Based Recurrent Neural Network Using Multi-Dimensional Data," *Revue Roumaine Des Sciences Techniques — Série Électrotechnique Et Énergétique,* vol.69, No.1, pp. 103-108, 2024, doi: 10.59277/rrst-ee.2024.1.18

[13] P. Kavitha, A. Ahilan, A. Gnanamalar, and M Usha, "Twin face recognition using a deep learning-based pixel difference network with edge maps," *Signal, Image and Video Processing,* vol. 19, no. 1, pp. 1-9, 2025, doi: 10.1007/s11760-024-03577-4

[14] NG. Rani, NH. Priya, A. Ahilan and N. Muthukumaran, "LV-YOLO: Logistic vehicle speed detection, and counting using deep Learning based YOLO network," *Signal, Image Video Process,* vol. 18, no. 10, pp. 7419-7429, 2024, doi: 10.1007/s11760-024-03404-w

[15] A. Aarthi Gopalakrishnan, Neelima, and C. Priya, "Deep Learning Model for Tracking Human Behavior in Supermarket Through CCTV Footage," *International Journal of Computer and Engineering Optimization,* vol. 02, no. 01, pp. 01-06, 2024.

[16] BDK. Patro. "Multi-label Classification of Retinal Diseases using Hybrid Vision Transformer," In 2024 15th *International Conference on Computing Communication and Networking Technologies (ICCCNT).* pp. 1-5, 2024, doi: 10.1109/icccnt61001.2024.10725227

[17] R. Arun, BK. Muthu, and A. Ahilan, "Deep vein thrombosis detection via combination of neural networks," *Biomed. Signal Process. Control.,* vol. 100, pp. 106972, 2025, doi: 10.1016/j.bspc.2024.106972

[18] A. Ahilan, M. Anlin Sahaya Tinu, A. Jasmine Gnana Malar, and B. Muthu Kumar, "Stationary Wavelet-Oriented Luminance Enhancement Approach for Brain Tumor Detection with Multi-modality Images," *In International Conference on Frontiers of Intelligent Computing: Theory and Applications,* pp. 461-473, 2023, doi: 10.1007/978-981-99-6702-5_38

[19] N. Sengar, RC. Joshi, MK. Dutta, and R. Burget, "EyeDeep-Net: a multi-class diagnosis of retinal diseases using deep neural network," *Neural Comput Appl*, vol. 35, no.14, pp. 10551-10571, 2023, doi: 10.1007/s00521-023-08249-x

[20] R. Sarki, K. Ahmed, H. Wang, Y. Zhang, and K. Wang, "Convolutional neural network for multi-class classification of diabetic eye disease," *EAI Endorsed Transactions on Scalable Information Systems*, vol. 9, no. 4, 2021, doi: 10.4108/eai.16-12-2021.172436

Manuscript Received 20 July 2025; Revised 10 September 2025; Accepted 20 September 2025; Available online 29 September 2025
Digital Object Identifier (**DOI**): https://doi.org/10.35882/jeeemi.v7i4.925

[21] N. Gour, and P Khanna, "Multi-class multi-label ophthalmological disease detection using transfer learning based convolutional neural network. Biomed," *Signal Process. Control.,* vol. 66, pp.102329, 2021, doi: 10.1016/j.bspc.2020.102329
[22] R. Sarki, K. Ahmed, H. Wang and Y. Zhang, "Automated detection of mild and multi-class diabetic eye diseases using deep learning," *Health Inf. Sci. Syst,* vol. 8, no. 1, pp. 32, 2020, doi: 10.1007/s13755-020-00125-5
[23] M.G. Gualsaqui, S.M. Cuenca, I.L. Rosero, D.A. Almeida, C. Cadena, F. Villalba, and J.D. Cruz, "Multi-class classification approach for retinal diseases," *Journal of Advances in Information Technology,* vol. 14, no. 3, pp.392-398. 2023, doi: 10.12720/jait.14.3.392-398
[24] T. Vaiyapuri, S. Srinivasan, M.Y. Sikkandar, T.S. Balaji, S. Kadry, M.N. Meqdad, and Y. Nam, "Intelligent Deep Learning Based Multi-Retinal Disease Diagnosis and Classification Framework," *Comput. Mater. Continua*., vol. 73, no. 3, 2022, doi: 10.32604/cmc.2022.023919
[25] J. Kim, and L. Tran, "Retinal disease classification from oct images using deep learning algorithms," In 2021 *IEEE Conference on Computational Intelligence in Bioinformatics and Computational Biology (CIBCB)*, IEEE, pp. 1-6, 2021, doi: 10.1109/cibcb49929.2021.9562919
[26] Z. Huang, X. Song, Z. Liao, and B. Jia, "Bearing Fault Feature Enhancement and Diagnosis Base on Savitzky-Golay Filtering Gramian Angular Field," *IEEE Access*, 2024, doi: 10.1109/access.2024.3418414
[27] M. Tan, and Q. Le, "Efficientnet: Rethinking model scaling for convolutional neural networks," *In International conference on machine learning*, pp. 6105-6114, 2019.
[28] Y. Wei, J. Jang-Jaccard, F. Sabrina, A. Singh, W. Xu, and S. Camtepe, Ae-mlp: A hybrid deep learning approach for ddos detection and classification," *IEEE Access*, vol. 9, pp. 146810-146821, 2021, doi: 10.1109/access.2021.3123791
[29] S. Pachade, P. Porwal, D. Thulkar, M. Kokare, G. Deshmukh, V. Sahasrabuddhe, L. Giancardo, G. Quellec, and F. Mériaudeau, "Retinal fundus multi-disease image dataset (rfmid): A dataset for multi-disease detection research," *Data*, vol. 6, no. 2, pp. 14, 2021.

Author Biography

Mohana Suganthi N currently holds the position of Assistant Professor in the Department of Computer Science and Engineering at Vel Tech Rangarajan Dr. Sagunthala R&D Institute of Science and Technology, nestled in Avadi, Chennai, Tamil Nadu. She earned her Bachelor of Engineering from the University of Madras in October 1995 and pursued further academic excellence by obtaining her Master of Engineering from Anna University in June 2013. Over more than a decade, she has diligently contributed to curriculum development, faculty mentorship, and institutional quality enhancement, including active participation in prestigious NBA and NAAC accreditation processes. Her research interests are wide-ranging, spanning advanced domains such as Machine Learning, Deep Learning, Data Science, and Cloud Computing. She has authored and co-authored numerous distinguished research articles in well-recognized, peer-reviewed journals and conference proceedings, significantly elevating both her professional standing and the scholarly reputation of her department.

Arun M is presently a Professor in the Department of Computer Science and Engineering at Vel Tech Rangarajan Dr. Sagunthala R&D Institute of Science and Technology in Avadi, Chennai. He earned his Ph.D. in Information and Communication Engineering from Anna University, Chennai. With approximately sixteen years of dedicated academic experience, Dr. Arun has made significant scholarly contributions. His research has been disseminated through prestigious journals published by IET, Taylor & Francis, Emerald, and IOS Press. Over the years, he has consistently enriched the academic environment through both his teaching and his publications in these esteemed outlets.

Manuscript Received 20 July 2025; Revised 10 September 2025; Accepted 20 September 2025; Available online 29 September 2025
Digital Object Identifier (**DOI**): https://doi.org/10.35882/jeeemi.v7i4.925